Available online at www.sciencedirect.com
ScienceDirect
Mechanism and Machine Theory 42 (2007) 1484–1498
Mechanism and Machine Theory
www.elsevier.com/locate/mechmt

Spatial 6*R* linkages based on the combination of two Goldberg 5*R* linkages

Y. Chen [a], Z. You [b,*]

[a] *School of Mechanical and Aerospace Engineering, Nanyang Technological University, Singapore 639798, Singapore*
[b] *Department of Engineering Science, University of Oxford, Oxford OX1 3 PJ, UK*

Received 25 August 2006; received in revised form 7 December 2006; accepted 15 December 2006
Available online 15 February 2007

Abstract

In this paper, we report the creation of a pair of 6*R* linkages by combining Goldberg 5*R* linkages. The new linkages are similar to the Bennett-joint 6*R* linkages proposed by Mavroidis and Roth. However, unlike the Bennett-joint 6*R* linkages, the Bennett ratio, defined as the ratio between the sinusoidal value of the twist over a link and the length of the link, is not necessarily to be the same for all of the six links. The geometric parameters of the new linkages are defined and the closure equations have been derived. Physical models of the new linkages were constructed which validates our derivation.

Keywords: Bennett linkage; Goldberg 5*R* linkage; Bennett-joint 6*R* linkage; Closure equation; 6*R* linkage

1. Introduction

Since Bennett published his acclaimed paper "a new mechanism" [1] which gave birth to the Bennett linkage, it has been found that a number of 3D overconstrained linkages can be regarded as the combination of several Bennett linkages, including the Myard linkage [2], the Goldberg 5*R* and 6*R* linkages [3], the Bennett-joint 6*R* linkage [4], the Dietmaier 6*R* linkage [5], Wohlhart's double-Goldberg linkages [6], to list just a few. A summery was provided by Chen [7].

The first reported overconstrained linkage based on the Bennett linkage is the Myard linkage [2]. Found in 1931, this overconstrained 5*R* linkage is plane-symmetric, for which the two 'rectangular' Bennett chains, with one pair of twists being $\pi/2$, are symmetrically placed before combining them. In 1943, Goldberg [3] described another 5*R* linkage constructed using the Bennett linkage. It was obtained by combining two Bennett linkages in such a way that a link common to both was removed and a pair of adjacent links were rigidly attached to each other. The techniques that he developed was commonly known as the *summation* of two Bennett loops to produce a 5*R* linkage, or the *subtraction* of a primary composite loop from another Bennett chain to form a

* Corresponding author. Tel.: +44 1865 273137; fax: +44 1865 283301.
E-mail address: zhong.you@eng.ox.ac.uk (Z. You).

0094-114X/$ - see front matter
doi:10.1016/j.mechmachtheory.2006.12.008

Notations

$a_{12},\ldots$	the length of a link as the distance between the axes of two neighbouring revolutes 1 and 2, etc.
a, b	constants for the length of the links
a, **b**, **c** and **d**	the superscripts to represent Bennett linkages **a**, **b**, **c** and **d**
e and **f**	superscripts to represent Goldberg 5*R* linkages
I, **II**	superscript to represent the newly found Cases I and II 6*R* linkages
K	constant in the closure equations for the Bennett linkages
k_B	the Bennett ratio
m	the superscript to represent Bennett linkages
$R_1, R_2,\ldots$	offsets at revolutes $1,2,\ldots$
$\alpha_{12},\ldots$	the twist of a link which is defined as the skewed angle between the axes of two neighbouring revolute joints 1 and 2, etc.
α, β	constants used to represent the skewed angles between the axes of two adjacent revolute joints
$\phi_1,\ldots$	the revolute variable at joint 1, etc. for the Goldberg 5*R* linkage
$v_1,\ldots$	the revolute variable at joint 1, etc. for the new 6*R* linkage
$\theta_1,\ldots$	the revolute variable at joint 1, etc. for the Bennett linkage

syncopated linkage, see Fig. 1. The Goldberg 5*R* linkage was generalised by Wohlhart [6]. Based on that, he developed a new 6*R* overconstrained linkage, commonly known as the Wohlhart double-Goldberg linkage. Its synthesis is achieved by coalescing two appropriately generalised Goldberg 5*R* linkages and by removing the two common links as illustrated in Fig. 2. In 1994, the Bennett-joint 6*R* linkage [4] was discovered by Mavroidis and Roth as a by-product of their effort to develop a systematic method to deal with overconstrained linkages, which in fact is a combination of two Bennett linkages with the same Bennett ratios and no common axis. In 1995, Dietmaier [5] discovered a new family of overconstrained 6*R* linkages with the aid of

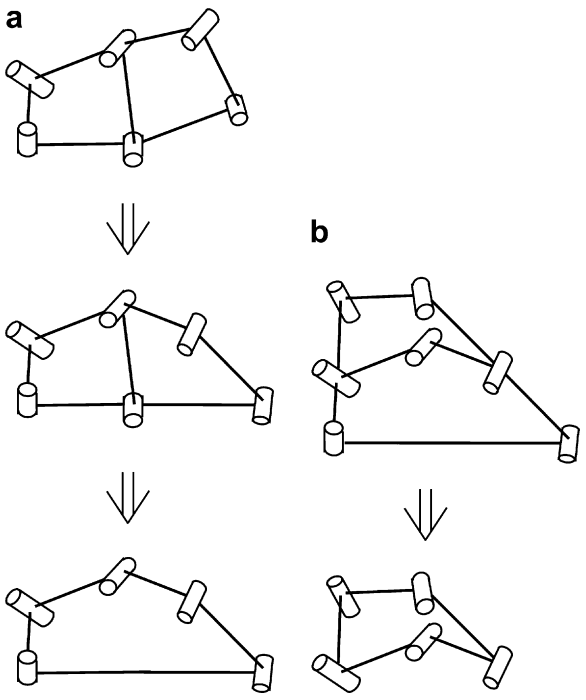

Fig. 1. Goldberg 5*R* linkages obtained by (a) summation and (b) subtraction.

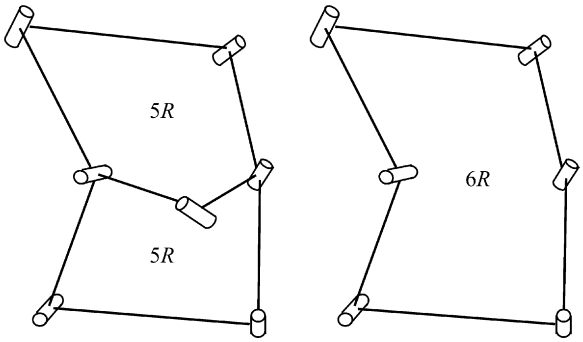

Fig. 2. Generation of a Wohlhart double-Goldberg linkage.

the numerical method, which extended the geometric condition of the Bennett-joint 6*R* linkage. More recently, Chen and Baker [8] and Baker [9] reported a class of 6*R* spatial linkage by combining a Bennett linkage with a planar 4*R* linkage following a method similar to that used to generate Waldron's hybrid overconstrained linkages previously [10].

In this paper, we report the discovery of a pair of new mechanisms obtained by combining two Goldberg 5*R* linkages. Similar to the Wohlhart double-Goldberg linkage we also use two Goldberg 5*R* linkages as building blocks. However, the Goldberg linkages are placed such that one link and portions of the other two links become common to both Goldberg linkages, instead of two common links as in Wohlhart's approach. We have proven that both of the resulted 6*R* linkages are also overconstrained and have in general single degree of mobility. One of the linkages has line-symmetry whereas the other one has not.

The layout of this paper is as follows. In Section 2, we briefly review the construction of two Goldberg 5*R* linkages using the Bennett linkages and their closure equations. Subsequently these Goldberg linkages are used for construction of the new 6*R* linkage. The relationships among the geometric parameters are defined and the closure equations are derived in Section 3. The characteristics of the newly found 6*R* linkages and its two possible formations are discussed in Section 4. The paper ends with some conclusions and further remarks in Section 5.

Note that in our derivation, the offset of the linkages is always zero because both Bennett linkage and Goldberg 5*R* linkage have zero offset. Possibility of having non-zero offsets is discussed in Section 5.

2. The Goldberg 5*R* linkage

We shall briefly review how two Goldberg 5*R* linkages can be built by summation [3]. Consider a set of four Bennett linkages **a**, **b**, **c** and **d**, which have the same Bennett ratio k_B, defined as the ratio between the sinusoidal value of twist and length of the same link [4]. Their geometric parameters and closure equations can be written as follows:

$$a_{12}^{\mathbf{m}} = a_{34}^{\mathbf{m}} = a^{\mathbf{m}}, \quad a_{23}^{\mathbf{m}} = a_{41}^{\mathbf{m}} = b^{\mathbf{m}}, \tag{1a}$$

$$\alpha_{12}^{\mathbf{m}} = \alpha_{34}^{\mathbf{m}} = \alpha^{\mathbf{m}}, \quad \alpha_{23}^{\mathbf{m}} = \alpha_{41}^{\mathbf{m}} = \beta^{\mathbf{m}}, \tag{1b}$$

$$\frac{\sin\alpha^{\mathbf{m}}}{a^{\mathbf{m}}} = \frac{\sin\beta^{\mathbf{m}}}{b^{\mathbf{m}}} = k_B \tag{1c}$$

and

$$\theta_1^{\mathbf{m}} + \theta_3^{\mathbf{m}} = 2\pi, \quad \theta_2^{\mathbf{m}} + \theta_4^{\mathbf{m}} = 2\pi, \tag{2a}$$

$$\tan\frac{\theta_1^{\mathbf{m}}}{2}\tan\frac{\theta_2^{\mathbf{m}}}{2} = \frac{\sin\frac{1}{2}(\alpha_{23}^{\mathbf{m}} + \alpha_{12}^{\mathbf{m}})}{\sin\frac{1}{2}(\alpha_{23}^{\mathbf{m}} - \alpha_{12}^{\mathbf{m}})} = \frac{\sin\frac{1}{2}(\beta^{\mathbf{m}} + \alpha^{\mathbf{m}})}{\sin\frac{1}{2}(\beta^{\mathbf{m}} - \alpha^{\mathbf{m}})} = K^{\mathbf{m}}, \tag{2b}$$

where $\mathbf{m} = \mathbf{a}$, **b**, **c** and **d**.

If

$$a^{\mathbf{a}} = a^{\mathbf{c}} \quad \text{and} \quad \alpha^{\mathbf{a}} = \alpha^{\mathbf{c}} \tag{3}$$

linkages **a** and **c** can be summated to form a Goldberg 5*R* linkage, **e**, as shown in Fig. 3. In the summation (or joining) of two linkages those links bridging hinges 1 and 2 in the Bennett linkages become the common link and links 23 in **a** and 41 in **c** are made co-linear and rigidly connected. The 5*R* linkage is obtained after the removal of the common link. The conditions on its geometric parameters for the newly formed Goldberg linkage **e** are as follows:

$$a^{\mathbf{e}}_{34} = a^{\mathbf{e}}_{12} + a^{\mathbf{e}}_{51} = b^{\mathbf{a}} + b^{\mathbf{c}}, \quad a^{\mathbf{e}}_{23} = a^{\mathbf{a}} = a^{\mathbf{c}} = a^{\mathbf{e}}_{45}, \tag{4a}$$

$$\alpha^{\mathbf{e}}_{34} = \alpha^{\mathbf{e}}_{12} + \alpha^{\mathbf{e}}_{51} = \beta^{\mathbf{a}} + \beta^{\mathbf{c}}, \quad \alpha^{\mathbf{e}}_{23} = \alpha^{\mathbf{a}} = \alpha^{\mathbf{c}} = \alpha^{\mathbf{e}}_{45}, \tag{4b}$$

and

$$\frac{\sin\alpha^{\mathbf{a}}}{a^{\mathbf{a}}} = \frac{\sin\beta^{\mathbf{a}}}{b^{\mathbf{a}}} = \frac{\sin\beta^{\mathbf{c}}}{b^{\mathbf{c}}} = k_{\mathrm{B}}. \tag{4c}$$

The new revolute variables are $\phi^{\mathbf{e}}_1, \phi^{\mathbf{e}}_2, \ldots, \phi^{\mathbf{e}}_5$. From Fig. 3, there are

$$\phi^{\mathbf{e}}_1 = \theta^{\mathbf{a}}_1 + \theta^{\mathbf{c}}_2 - \pi, \quad \phi^{\mathbf{e}}_2 = \theta^{\mathbf{c}}_3, \quad \phi^{\mathbf{e}}_3 = \theta^{\mathbf{c}}_4, \quad \phi^{\mathbf{e}}_4 = \theta^{\mathbf{a}}_3 \quad \text{and} \quad \phi^{\mathbf{e}}_5 = \theta^{\mathbf{a}}_4.$$

The closure equations are [11]

$$\phi^{\mathbf{e}}_1 + \phi^{\mathbf{e}}_3 + \phi^{\mathbf{e}}_4 = 3\pi, \tag{5a}$$

$$\phi^{\mathbf{e}}_2 + \phi^{\mathbf{e}}_5 = 3\pi, \tag{5b}$$

$$\tan\frac{\phi^{\mathbf{e}}_2}{2}\tan\frac{\phi^{\mathbf{e}}_3}{2} = K^{\mathbf{c}}, \tag{5c}$$

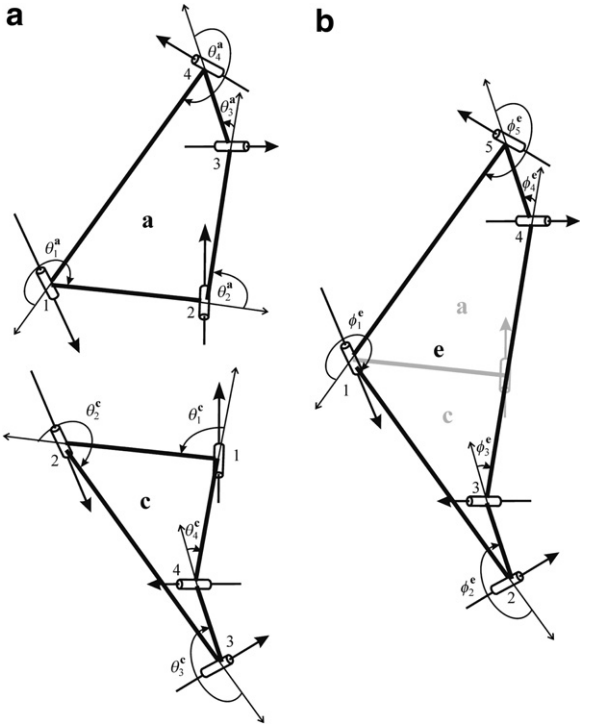

Fig. 3. Formation of a Goldberg 5*R* linkage from two Bennett linkages. (a) Bennett linkages **a** and **c**. (b) Summation of **a** and **c** forms Goldberg 5*R* linkage **e**.

and

$$\tan\frac{\phi_4^{\mathbf{e}}}{2}\tan\frac{\phi_5^{\mathbf{e}}}{2}=K^{\mathbf{a}}. \tag{5d}$$

Considering Eqs. (5b)–(5d) yields

$$\tan\frac{\phi_3^{\mathbf{e}}}{2}\tan\frac{\phi_4^{\mathbf{e}}}{2}=K^{\mathbf{a}}K^{\mathbf{c}}. \tag{5e}$$

Similarly, Bennett linkages **b** and **d** can be summated into a Goldberg 5*R* linkage, **f**, as show in Fig. 4, provided that

$$a^{\mathbf{b}}=a^{\mathbf{d}} \quad \text{and} \quad \alpha^{\mathbf{b}}=\alpha^{\mathbf{d}}. \tag{6}$$

The conditions on its geometric parameters are similar to those shown in Eq. (4)

$$a_{34}^{\mathbf{f}}=a_{12}^{\mathbf{f}}+a_{51}^{\mathbf{f}}=b^{\mathbf{b}}+b^{\mathbf{d}}, \quad a_{23}^{\mathbf{f}}=a_{45}^{\mathbf{f}}=a^{\mathbf{b}}, \tag{7a}$$

$$\alpha_{34}^{\mathbf{f}}=\alpha_{12}^{\mathbf{f}}+\alpha_{51}^{\mathbf{f}}=\beta^{\mathbf{b}}+\beta^{\mathbf{d}}, \quad \alpha_{23}^{\mathbf{f}}=\alpha_{45}^{\mathbf{f}}=\alpha^{\mathbf{b}}, \tag{7b}$$

and

$$\frac{\sin\alpha^{\mathbf{b}}}{a^{\mathbf{b}}}=\frac{\sin\beta^{\mathbf{b}}}{b^{\mathbf{b}}}=\frac{\sin\beta^{\mathbf{d}}}{b^{\mathbf{d}}}=k_{\mathrm{B}}. \tag{7c}$$

Denote the revolute variables by $\phi_1^{\mathbf{f}},\phi_2^{\mathbf{f}},\ldots,\phi_5^{\mathbf{f}}$. From Fig. 4,

$$\phi_1^{\mathbf{f}}=\theta_4^{\mathbf{b}}+\theta_3^{\mathbf{d}}-\pi, \quad \phi_2^{\mathbf{f}}=\theta_1^{\mathbf{b}}, \quad \phi_3^{\mathbf{f}}=\theta_2^{\mathbf{b}}, \quad \phi_4^{\mathbf{f}}=\theta_1^{\mathbf{d}} \quad \text{and} \quad \phi_5^{\mathbf{f}}=\theta_2^{\mathbf{d}}.$$

The closure equations are

$$\phi_1^{\mathbf{f}}+\phi_3^{\mathbf{f}}+\phi_4^{\mathbf{f}}=3\pi, \tag{8a}$$

$$\phi_2^{\mathbf{f}}+\phi_5^{\mathbf{f}}=3\pi, \tag{8b}$$

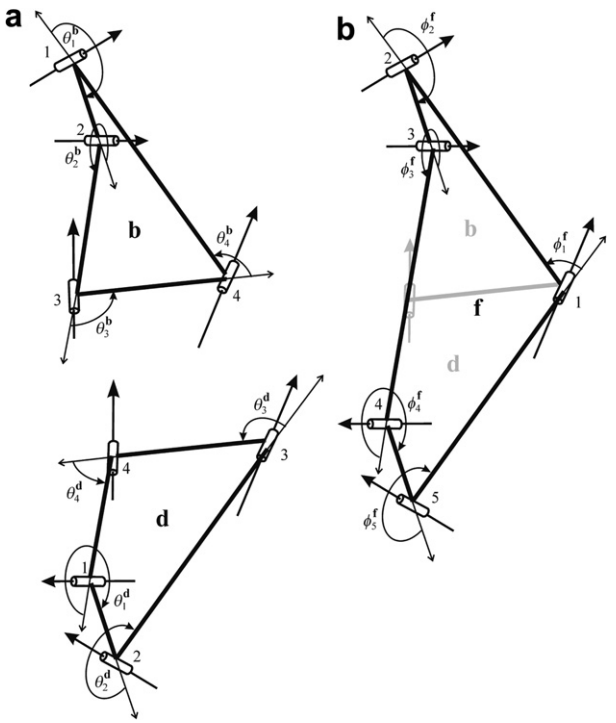

Fig. 4. Formation of the other Goldberg 5*R* linkage from two Bennett linkages. (a) Bennett linkages **b** and **d**. (b) Summation of **b** and **d** forms Goldberg 5*R* linkage **f**.

$$\tan\frac{\phi_2^{\mathbf{f}}}{2}\tan\frac{\phi_3^{\mathbf{f}}}{2}=K^{\mathbf{b}}, \tag{8c}$$

$$\tan\frac{\phi_4^{\mathbf{f}}}{2}\tan\frac{\phi_5^{\mathbf{f}}}{2}=K^{\mathbf{d}}, \tag{8d}$$

and

$$\tan\frac{\phi_3^{\mathbf{f}}}{2}\tan\frac{\phi_4^{\mathbf{f}}}{2}=K^{\mathbf{b}}K^{\mathbf{d}}, \tag{8e}$$

which is obtained by considering (8b)–(8d).

3. New 6*R* linkages

3.1. Geometric conditions

A new 6*R* linkage can be obtained by combining Goldberg linkages **e** and **f** using a particular layout shown in Fig. 5 in which link 34 in **e** and link 34 in **f** become the common link, and portions of links 23 and 45 in **e**

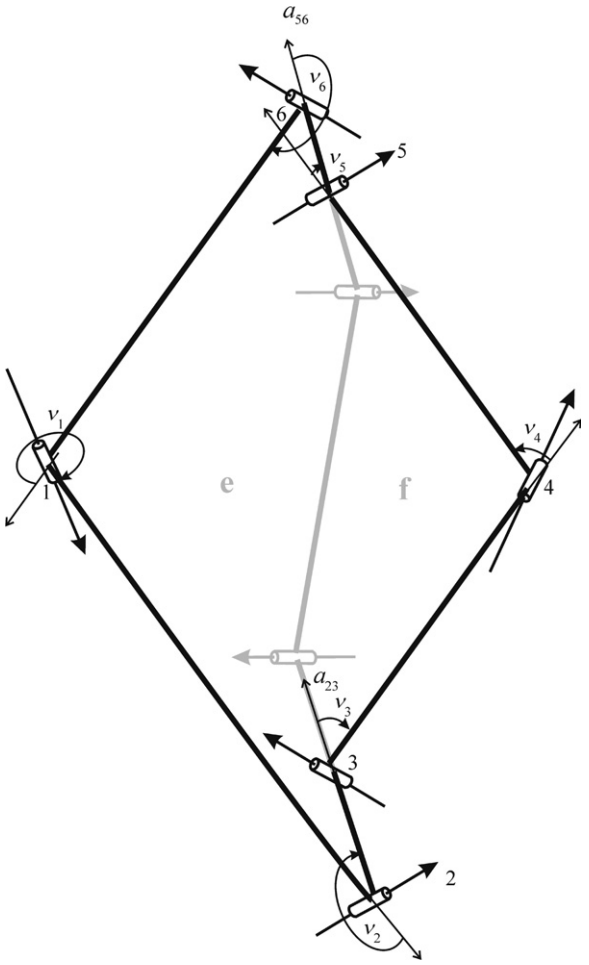

Fig. 5. A 6*R* linkage constructed from two Goldberg 5*R* linkages **e** and **f**. Parts in grey are common to both Goldberg linkages and they are subsequently removed.

overlap with links 45 and 23 of **f**, respectively. To enable such connection, the following conditions must be met:

(a) Link 34 of **e** and link 34 of **f** are the same link, i.e.

$$a_{34}^{\mathbf{e}} = a_{34}^{\mathbf{f}}. \tag{9a}$$

(b) Joints 3 and 4 of **e** should be the same as joints 4 and 3 of **f**, respectively, i.e.

$$\alpha_{34}^{\mathbf{e}} = \alpha_{34}^{\mathbf{f}}. \tag{9b}$$

(c) Link 45 of **e** and link 23 of **f** ought to have the same motion, so do link 23 of **e** and link 45 of **f**, i.e.

$$\phi_3^{\mathbf{e}} + \phi_4^{\mathbf{f}} = 2\pi \quad \text{and} \quad \phi_3^{\mathbf{f}} + \phi_4^{\mathbf{e}} = 2\pi. \tag{9c}$$

Conditions (9a) and (9b) can be readily replaced by more explicit expressions. Bearing in mind that the Goldberg linkages **e** and **f** are made from Bennett linkages **a**, **c** and **b**, **d**, respectively, Eq. (9a) can be written as

$$b^{\mathbf{a}} + b^{\mathbf{c}} = b^{\mathbf{b}} + b^{\mathbf{d}} \tag{10}$$

due to Eqs. (4a) and (7a). This equation can also be written in terms of β's using (1c). There is

$$\sin\beta^{\mathbf{a}} + \sin\beta^{\mathbf{c}} = \sin\beta^{\mathbf{b}} + \sin\beta^{\mathbf{d}}. \tag{11}$$

Similarly, because of Eqs. (4b) and (7b), (9b) becomes

$$\beta^{\mathbf{a}} + \beta^{\mathbf{c}} = \beta^{\mathbf{b}} + \beta^{\mathbf{d}}. \tag{12}$$

Two sets of β's exist that satisfy both Eqs. (11) and (12), which are

$$\beta^{\mathbf{a}} = \beta^{\mathbf{d}}, \quad \beta^{\mathbf{b}} = \beta^{\mathbf{c}} \tag{13}$$

and

$$\beta^{\mathbf{a}} = \beta^{\mathbf{b}}, \quad \beta^{\mathbf{c}} = \beta^{\mathbf{d}}, \tag{14}$$

provided that all of the twists are confined within $(0, \pi)$.

Taking conditions (13), (14) as well as (3) and (6) into account, it becomes apparent that two sets of geometries exist for **e** and **f** to be combined into a 6*R* linkage. So effectively we have obtained *two* linkages, which are summarised in Table 1 as the Cases I and II linkages. Fig. 6a shows both linkages. Case I of the linkage is the loop linking revolutes 1, 2, 3, 4 (in grey), 5, 6 and back to 1, whereas Case II of the linkage is the loop from revolutes 1, 2, 3, 4 (in black), 5, 6 and back to 1.

A diagram, showing the difference between Cases I and II, is given in Fig. 6b.

Careful readers may have noticed that so far we have not elaborated condition (9c). In fact, it forges a link between α and β. The proof is as follows.

Table 1
Geometrical parameters of two cases of the new 6*R* linkage

	a_{12}	a_{23}	a_{34}	a_{45}	a_{56}	a_{61}
Case I	$b^{\mathbf{c}}$	$a^{\mathbf{a}} - a^{\mathbf{b}}$	$b^{\mathbf{a}}$	$b^{\mathbf{c}}$	$a^{\mathbf{a}} - a^{\mathbf{b}}$	$b^{\mathbf{a}}$
Case II			$b^{\mathbf{c}}$	$b^{\mathbf{a}}$		
	α_{12}	α_{23}	α_{34}	α_{45}	α_{56}	α_{61}
Case I	$\beta^{\mathbf{c}}$	$\alpha^{\mathbf{a}} - \alpha^{\mathbf{b}}$	$\beta^{\mathbf{a}}$	$\beta^{\mathbf{c}}$	$\alpha^{\mathbf{a}} - \alpha^{\mathbf{b}}$	$\beta^{\mathbf{a}}$
Case II			$\beta^{\mathbf{c}}$	$\beta^{\mathbf{a}}$		
	$\frac{\sin\alpha_{12}}{a_{12}}$	$\frac{\sin\alpha_{23}}{a_{23}}$	$\frac{\sin\alpha_{34}}{a_{34}}$	$\frac{\sin\alpha_{45}}{a_{45}}$	$\frac{\sin\alpha_{56}}{a_{56}}$	$\frac{\sin\alpha_{61}}{a_{61}}$
Case I	k_{B}	$k_{\mathrm{B}} \cdot \frac{\cos[(\beta^{\mathbf{c}} + \beta^{\mathbf{a}})/2]}{\cos[(\beta^{\mathbf{c}} - \beta^{\mathbf{a}})/2]}$	k_{B}	k_{B}	$k_{\mathrm{B}} \cdot \frac{\cos[(\beta^{\mathbf{c}} + \beta^{\mathbf{a}})/2]}{\cos[(\beta^{\mathbf{c}} - \beta^{\mathbf{a}})/2]}$	k_{B}
Case II						

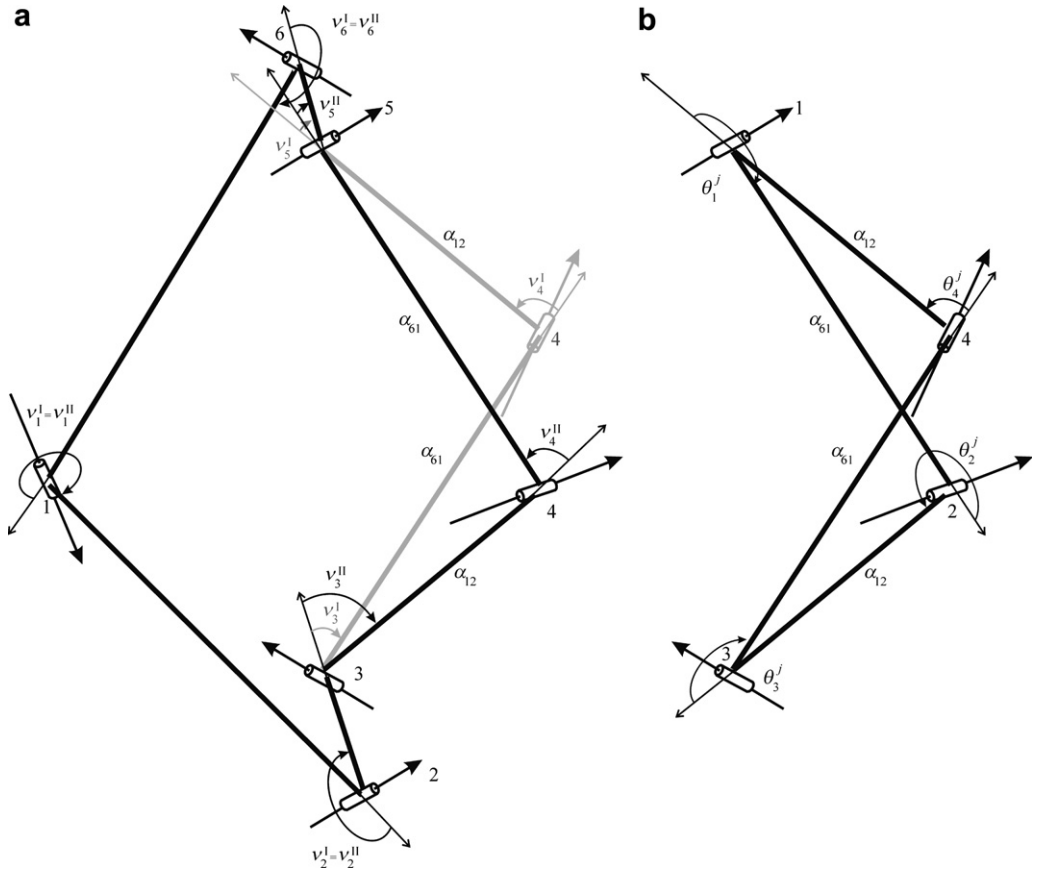

Fig. 6. The 6*R* linkages in Case I and Case II. (a) Linkages with both cases shown and (b) the difference between Cases I and II linkages is a Bennett linkage.

Firstly, combining conditions (9c) with (5e) and (8e) yields

$$K^{\mathbf{a}}K^{\mathbf{c}} = K^{\mathbf{b}}K^{\mathbf{d}},$$

which leads to the following condition for both Cases I and II:

$$\frac{\sin\frac{1}{2}(\beta^{\mathbf{a}}+\alpha^{\mathbf{a}})}{\sin\frac{1}{2}(\beta^{\mathbf{a}}-\alpha^{\mathbf{a}})}\cdot\frac{\sin\frac{1}{2}(\beta^{\mathbf{c}}+\alpha^{\mathbf{a}})}{\sin\frac{1}{2}(\beta^{\mathbf{c}}-\alpha^{\mathbf{a}})}=\frac{\sin\frac{1}{2}(\beta^{\mathbf{c}}+\alpha^{\mathbf{b}})}{\sin\frac{1}{2}(\beta^{\mathbf{c}}-\alpha^{\mathbf{b}})}\cdot\frac{\sin\frac{1}{2}(\beta^{\mathbf{a}}+\alpha^{\mathbf{b}})}{\sin\frac{1}{2}(\beta^{\mathbf{a}}-\alpha^{\mathbf{b}})}.$$

Then applying some trigonometric manipulation, the above equation becomes

$$\tan\frac{\alpha^{\mathbf{a}}}{2}\tan\frac{\alpha^{\mathbf{b}}}{2}=\tan\frac{\beta^{\mathbf{a}}}{2}\tan\frac{\beta^{\mathbf{c}}}{2}. \tag{15}$$

3.2. The closure equations

Now we are to derive the closure equations for the new 6*R* linkage. We start with Case I of the linkage.

Denote revolute variables of the new Case I 6*R* linkage by $v_1^{\mathbf{I}}, v_2^{\mathbf{I}}, \ldots, v_6^{\mathbf{I}}$. They can be expressed in terms of those revolute variables for Goldberg linkages **e** and **f** such that

$$v_1^{\mathbf{I}} = \phi_1^{\mathbf{e}}, \tag{16a}$$
$$v_2^{\mathbf{I}} = \phi_2^{\mathbf{e}}, \tag{16b}$$
$$v_3^{\mathbf{I}} = \phi_5^{\mathbf{f}} - \pi, \tag{16c}$$
$$v_4^{\mathbf{I}} = \phi_1^{\mathbf{f}}, \tag{16d}$$
$$v_5^{\mathbf{I}} = \phi_2^{\mathbf{f}} - \pi \tag{16e}$$

and

$$v_6^{\mathbf{I}} = \phi_5^{\mathbf{e}}. \tag{16f}$$

By combining Eqs. (5a), (8a), (9c), (16a) and (16d), we obtain

$$v_1^{\mathbf{I}} + v_4^{\mathbf{I}} = 2\pi. \tag{17a}$$

Considering Eqs. (5b), (16b) and (16f) yields,

$$v_2^{\mathbf{I}} + v_6^{\mathbf{I}} = 3\pi. \tag{17b}$$

From Eqs. (8b), (16c) and (16e), there is

$$v_3^{\mathbf{I}} + v_5^{\mathbf{I}} = \pi. \tag{17c}$$

Bringing together Eqs. (5c), (8d), (9c), (16b) and (16c) produces,[1]

$$\tan\frac{v_2^{\mathbf{I}}}{2} \cdot \tan\frac{v_3^{\mathbf{I}}}{2} = \frac{K^{\mathbf{c}}}{K^{\mathbf{d}}} = -1.$$

The above equation is equivalent to[2]

$$v_2^{\mathbf{I}} = v_3^{\mathbf{I}} + \pi. \tag{17d}$$

Now let us derive the last enclosure equation. From (5a), we can have

$$\tan\frac{1}{2}(3\pi - \phi_1^{\mathbf{e}}) = \tan\frac{1}{2}(\phi_3^{\mathbf{e}} + \phi_4^{\mathbf{e}}).$$

Due to Eqs. (5c), (5d) and (5e), the above equation becomes

$$\frac{1}{\tan\frac{\phi_1^{\mathbf{e}}}{2}} = \frac{\frac{K^{\mathbf{c}}}{\tan\frac{\phi_2^{\mathbf{e}}}{2}} + \frac{K^{\mathbf{a}}}{\tan\frac{\phi_5^{\mathbf{e}}}{2}}}{1 - K^{\mathbf{a}}K^{\mathbf{c}}}.$$

Because of (16a), (16b), (16f), and (17b), we can obtain that

$$\tan\frac{v_1^{\mathbf{I}}}{2} = \frac{(1 - K^{\mathbf{a}}K^{\mathbf{c}})\tan\frac{v_2^{\mathbf{I}}}{2}}{K^{\mathbf{c}} + K^{\mathbf{a}}\tan^2\frac{v_2^{\mathbf{I}}}{2}}.$$

Noted that $K^{\mathbf{a}}$ and $K^{\mathbf{c}}$ can be expressed in terms of $\alpha^{\mathbf{a}}$, $\beta^{\mathbf{a}}$ and $\beta^{\mathbf{c}}$. We can also replace them by the skewed angles of the new 6R linkage using Table 1. Thus, the above equation can be rewritten as follows:

$$\tan\frac{v_1^{\mathbf{I}}}{2} = \frac{\sin\frac{1}{2}(\alpha_{12} + \alpha_{61})\sin v_2^{\mathbf{I}}}{\tan\frac{\alpha_{56}}{2}\cos\frac{1}{2}(\alpha_{12} - \alpha_{61}) + \sin\frac{1}{2}(\alpha_{12} - \alpha_{61})\cos v_2^{\mathbf{I}}}. \tag{17e}$$

Eqs. (17a)–(17d) and (17e) are the five closure equations of the new 6R linkage, which also shows that this linkage has generally only one degree of mobility.

Now consider the Case II 6R linkage. A close inspection of its geometric parameters given in Table 1 reveals that in the two cases the length and twist of links 34 and 45 are switched over. Image that a linkage is built

[1] It can be shown that $\frac{K^{\mathbf{c}}}{K^{\mathbf{d}}} = \frac{\sin\frac{1}{2}(\beta^{\mathbf{c}}+\alpha^{\mathbf{a}})}{\sin\frac{1}{2}(\beta^{\mathbf{c}}-\alpha^{\mathbf{a}})} \cdot \frac{\sin\frac{1}{2}(\beta^{\mathbf{a}}-\alpha^{\mathbf{b}})}{\sin\frac{1}{2}(\beta^{\mathbf{a}}+\alpha^{\mathbf{b}})} = \frac{(\tan\frac{\beta^{\mathbf{a}}}{2}\tan\frac{\beta^{\mathbf{c}}}{2} - \tan\frac{\alpha^{\mathbf{a}}}{2}\tan\frac{\alpha^{\mathbf{b}}}{2}) - (\tan\frac{\beta^{\mathbf{c}}}{2}\tan\frac{\alpha^{\mathbf{b}}}{2} - \tan\frac{\beta^{\mathbf{a}}}{2}\tan\frac{\alpha^{\mathbf{a}}}{2})}{(\tan\frac{\beta^{\mathbf{a}}}{2}\tan\frac{\beta^{\mathbf{c}}}{2} - \tan\frac{\alpha^{\mathbf{a}}}{2}\tan\frac{\alpha^{\mathbf{b}}}{2}) + (\tan\frac{\beta^{\mathbf{c}}}{2}\tan\frac{\alpha^{\mathbf{b}}}{2} - \tan\frac{\beta^{\mathbf{a}}}{2}\tan\frac{\alpha^{\mathbf{a}}}{2})} = -1$ owing to Eq. (15).

[2] Similarly we can show that $v_6^{\mathbf{I}} = v_5^{\mathbf{I}} + \pi$. However, this is not an independent closure equation.

with links 34 and 45 of both cases as shown in Fig. 6a. In this linkage links 34 and 45 and joint 4 in black belong to Case II whereas those in grey belong to Case I. It is very interesting to note that these four links actually form a Bennett linkage, see Fig. 6b, with lengths a_{12}, a_{61} and twists α_{12}, α_{61}. Hence, a Case II 6*R* linkage can be regarded as the combination of a Case I 6*R* linkage and a Bennett linkage after the removal of the common links and the joint. Thus, the closure equations of a Case II 6*R* linkage can be derived either by following the same step as we did for Case I or from those of the Case I 6*R* linkage and that of the Bennett linkage. They are listed as follows:

$$v_1^{\mathbf{II}} + v_4^{\mathbf{II}} = 2\pi, \tag{18a}$$

$$v_2^{\mathbf{II}} + v_6^{\mathbf{II}} = 3\pi, \tag{18b}$$

$$v_3^{\mathbf{II}} + v_5^{\mathbf{II}} = \pi, \tag{18c}$$

$$\tan\frac{v_2^{\mathbf{II}}}{2}\tan\frac{v_3^{\mathbf{II}}}{2} = \frac{\tan\frac{1}{2}(\alpha_{12}-\alpha_{61}) + \tan\frac{\alpha_{56}}{2}}{\tan\frac{1}{2}(\alpha_{12}-\alpha_{61}) - \tan\frac{\alpha_{56}}{2}}, \tag{18d}$$

and

$$\tan\frac{v_1^{\mathbf{II}}}{2} = \frac{\sin\frac{1}{2}(\alpha_{12}+\alpha_{61})\sin v_2^{\mathbf{II}}}{\tan\frac{\alpha_{56}}{2}\cos\frac{1}{2}(\alpha_{12}-\alpha_{61}) + \sin\frac{1}{2}(\alpha_{12}-\alpha_{61})\cos v_2^{\mathbf{II}}}. \tag{18e}$$

3.3. Models

We can use Table 1 to construct the new linkages. The procedures can be summarised as follows:

(a) Determine a_{12}, a_{61}, a_{23} and α_{12}.
(b) Calculate k_{B}.
(c) Obtain α_{61}.
(d) Calculate $k_{\mathrm{B}} \cdot \frac{\cos[(\alpha_{12}+\alpha_{61})/2]}{\cos[(\alpha_{12}-\alpha_{61})/2]}$.
(e) Get α_{23}.

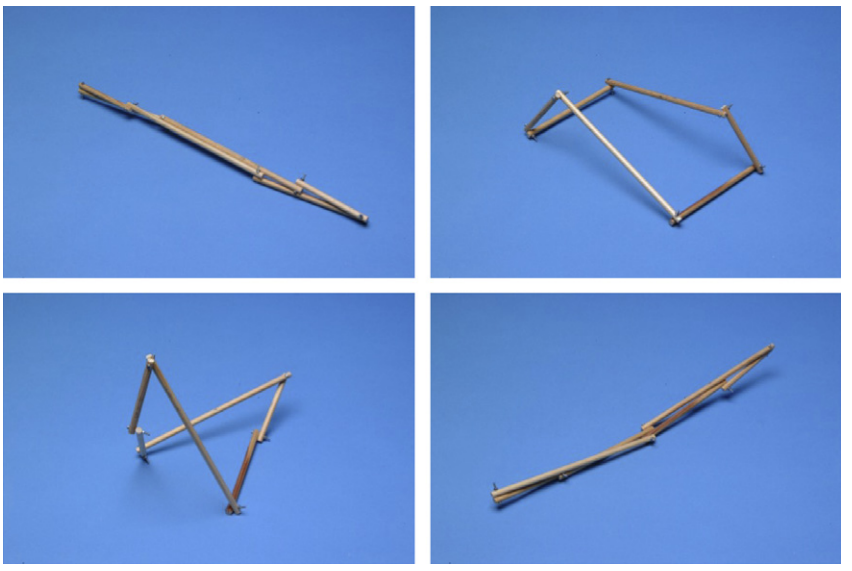

Fig. 7. Motion sequence of a model of the Case I 6*R* linkage.

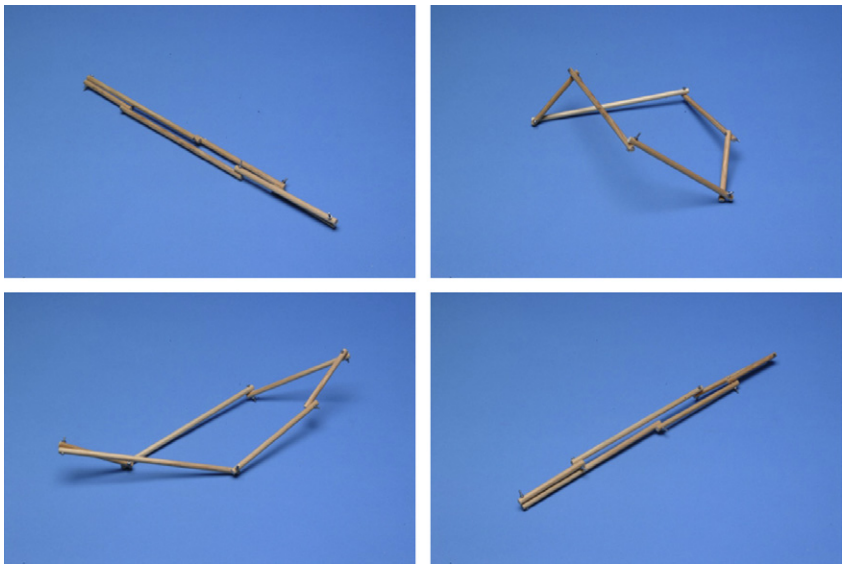

Fig. 8. Motion sequence of a model of the Case II 6*R* linkage.

Two models were constructed for the Cases I and II linkages, respectively. For the Case I linkage model,

$$a_{12} = a_{45} = 111.3\text{ mm};\quad a_{34} = a_{61} = 170.6\text{ mm};\quad a_{23} = a_{56} = 68.4\text{ mm};$$
$$\alpha_{12} = \alpha_{45} = 2/9\pi;\quad \alpha_{34} = \alpha_{61} = 5/9\pi,\quad \text{and}\quad \alpha_{23} = \alpha_{56} = 23/45\pi.$$

whereas for the Case II linkage model,

$$a_{12} = a_{34} = 111.3\text{ mm};\quad a_{45} = a_{61} = 170.6\text{ mm};\quad a_{23} = a_{56} = 68.4\text{ mm};$$
$$\alpha_{12} = \alpha_{34} = 2/9\pi;\quad \alpha_{45} = \alpha_{61} = 5/9\pi,\quad \text{and}\quad \alpha_{23} = \alpha_{56} = 23/45\pi.$$

The motion sequences of the models are shown in Figs. 7 and 8, respectively.

4. Characteristics of 6*R* linkage

4.1. Case I linkages

The characteristics of the newly found 6*R* linkage is best illustrated by some examples. First, consider a linkage where $\alpha_{12} = 2\pi/9$, $\alpha_{61} = 5\pi/9$ and thus $\alpha_{12} - \alpha_{61} = \pi/3$. Now let

(a) $\alpha_{56} = 5\pi/9 > \alpha_{12} - \alpha_{61}$,
(b) $\alpha_{56} = \pi/3 = \alpha_{12} - \alpha_{61}$,
(c) $\alpha_{56} = \pi/6 < \alpha_{12} - \alpha_{61}$.

The $v_2^{\mathbf{I}}$ vs. $v_1^{\mathbf{I}}$ curves of the linkage can be obtained using Eq. (17e) and are shown in Fig. 9. It becomes apparent that all of the links in the linkage can become co-linear when $v_1^{\mathbf{I}}$ and $v_2^{\mathbf{I}}$ become $(0, \pi)$ because other revolute variables will be either 0 or π due to Eqs. (17a)–(17c) and (17d). Besides, in (b), both $v_1^{\mathbf{I}}$ and $v_2^{\mathbf{I}}$ can reach $(\pi, 0)$. This is an additional configuration where the links become co-linear. In (c), $v_1^{\mathbf{I}}$ reaches π when $v_2^{\mathbf{I}} = \arccos\left(\frac{\tan\frac{\alpha_{56}}{2}}{\tan\frac{1}{2}|\alpha_{12}-\alpha_{61}|}\right)$ and $v_2^{\mathbf{I}} = 2\pi - \arccos\left(\frac{\tan\frac{\alpha_{56}}{2}}{\tan\frac{1}{2}|\alpha_{12}-\alpha_{61}|}\right)$. The linkage can partially closed, i.e., some of the links can become co-linear.

Secondly, consider a linkage with $\alpha_{12} = \alpha_{61}$. Eq. (17e) becomes

$$\tan\frac{v_1^{\mathbf{I}}}{2} = \frac{\sin\alpha_{12}}{\tan\frac{\alpha_{56}}{2}} \cdot \sin v_2^{\mathbf{I}}.$$

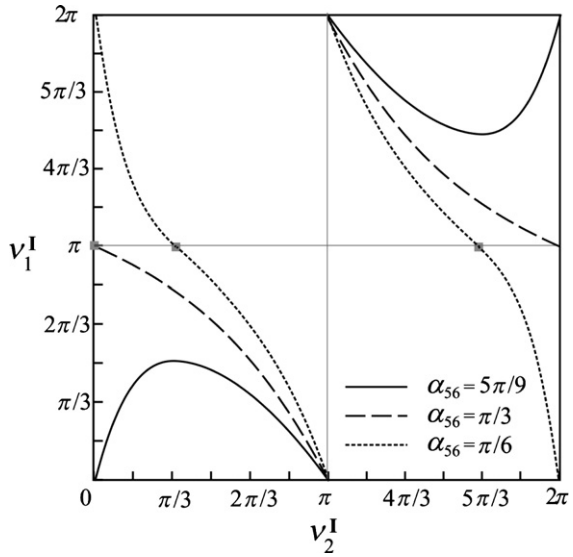

Fig. 9. v_1^I vs. v_2^I curves of the Case I 6*R* linkage for three different α_{56} when $\alpha_{12} = 2\pi/9$ and $\alpha_{61} = 5\pi/9$.

The v_2^I vs. v_1^I curves are plotted in Fig. 10. They are similar to those with $\alpha_{56} > \alpha_{12} - \alpha_{61}$ where v_1^I never reaches π under any circumstances. The maximum value of v_1^I is obtained when $v_2^I = \pi/2$ or $3\pi/2$. The movement of the linkage is restricted in comparison with other designs owing to the range of angles that v_1^I may reach.

Thirdly, it is interesting to note that motion bifurcation occurs when six links are co-linear. Although seemingly the input–output curves are uniquely defined for each given set of twists, two sets of the curves are in fact for the same physical models. For instance, $\alpha_{56} = \pi/6$ and $\alpha_{56} = \pi/6 + \pi = 7\pi/6$ correspond to the same model. The only difference is that the direction of the axis of the revolute joint 5 or 6 is selected differently.

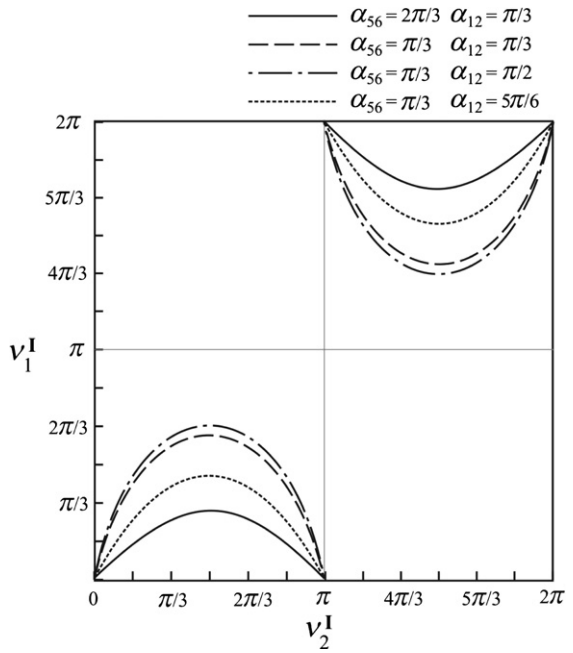

Fig. 10. v_1^I vs. v_2^I curves of the Case I 6*R* linkage when $\alpha_{12} = \alpha_{61}$.

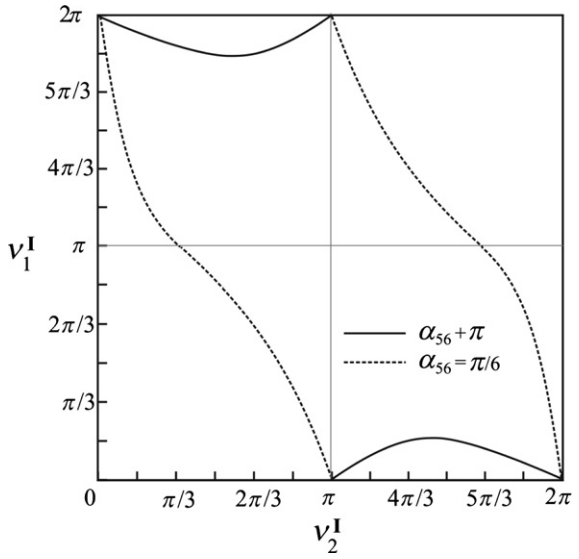

Fig. 11. Motion bifurcation of a Case I linkage at $v_1^{\mathbf{I}} = 0$, $v_2^{\mathbf{I}} = \pi$ and at $v_1^{\mathbf{I}} = 0$, $v_2^{\mathbf{I}} = 0$.

Thus, the motion may switch from one curve for $\alpha_{56} = \pi/6$ to that for $\alpha_{56} = 7\pi/6$ at $v_1^{\mathbf{I}} = 0$ and $v_2^{\mathbf{I}} = \pi$, see Fig. 11. The same happens at $v_1^{\mathbf{I}} = 0$ and $v_2^{\mathbf{I}} = 0$.

Bifurcation of the motion can also be determined by analysing the state of self-stress of the 6*R* linkage in these configurations [12–14]. It is found that the number of states of self-stress increases to two, indicating the existence of bifurcation at $v_1^{\mathbf{I}} = 0$, $v_2^{\mathbf{I}} = \pi$ and at $v_1^{\mathbf{I}} = 0$, $v_2^{\mathbf{I}} = 0$.

4.2. Case II linkages

The input–output curves of v_1, v_4 and v_6 vs. v_2 are the identical for both linkages, whereas v_3 and v_5 vs. v_2 curves are different. For example, for the models shown in Figs. 7 and 8, the input–output functions are plotted in Fig. 12. The $v_1^{\mathbf{I}}$, $v_4^{\mathbf{I}}$, and $v_6^{\mathbf{I}}$ vs. $v_2^{\mathbf{I}}$ curves are identical to $v_1^{\mathbf{II}}$, $v_4^{\mathbf{II}}$, and $v_6^{\mathbf{II}}$ vs. $v_2^{\mathbf{II}}$ curves, see Fig. 12a, whereas the $v_3^{\mathbf{I}}$ and $v_5^{\mathbf{I}}$ vs. $v_2^{\mathbf{I}}$ curves noticeably different from the comparable curves of $v_3^{\mathbf{II}}$ and $v_5^{\mathbf{II}}$ vs. $v_2^{\mathbf{II}}$, as shown in Fig. 12b.

For the Case II linkage kinematic bifurcation also occurs at $v_1^{\mathbf{II}} = 0$, $v_2^{\mathbf{II}} = 0$, and $v_1^{\mathbf{II}} = 0$, $v_2^{\mathbf{II}} = \pi$.

5. Conclusions and further discussion

In this paper, two new 6*R* linkages, namely Cases I and II linkages, have been created by summation of Goldberg 5*R* linkages. The difference between the two newly found linkages is a Bennett linkage. Closure equations for the linkages have been derived. Both of the linkages exhibit motion bifurcations when all of the links become co-linear.

A close inspection of the geometric parameters and the input–output curves reveals that the Case I linkage has a symmetric line, which is perpendicular to the three connection lines linking joints 1 and 4, joints 2 and 5, as well as joints 3 and 6, respectively. This is quite obvious in the second photograph in Fig. 7. However, the same cannot be said about the Case II linkage. It is completely non-symmetric. The relationships among the geometric parameters of the Cases I and II linkages are very similar to those of the Bennett-joint 6*R* linkage [4], which also has a line-symmetric and a non-symmetric case. But in the Bennett-joint 6*R* linkage, all of the links have the same Bennett ratio, k_B, whereas in the Cases I and II linkages, links 23 and 56 have the different Bennett ratio. In fact, both the line-symmetric Bennett-joint 6*R* linkage and Case I linkage are the two special cases of Bricard line-symmetric linkage [15]. Therefore, we envisage that the zero offsets of the Case I 6*R* linkage could be replaced by

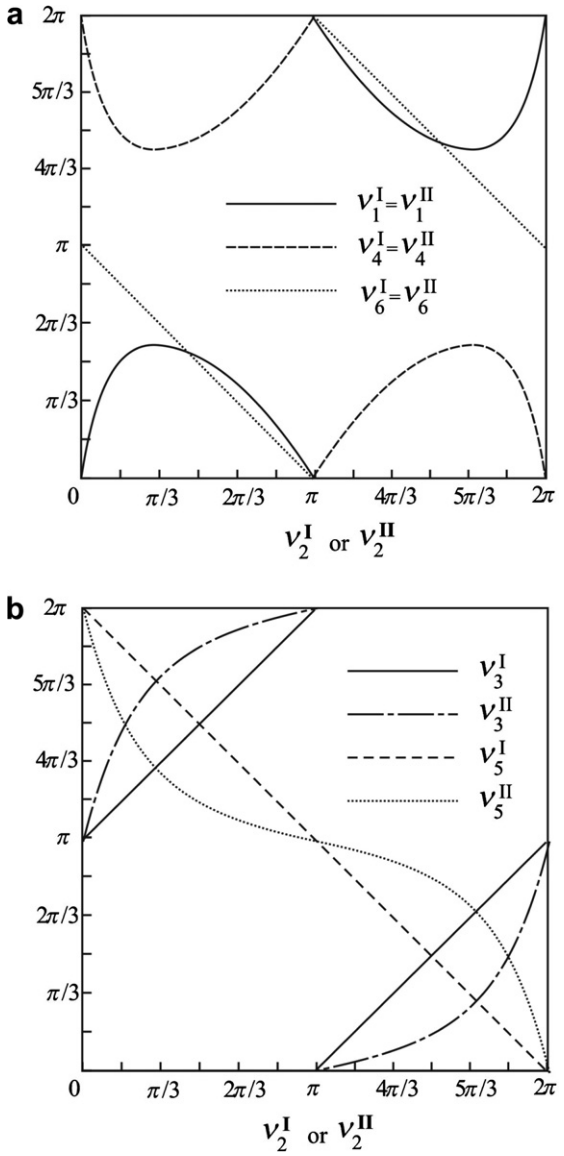

Fig. 12. The input–output functions of both Cases I and II linkage models shown in Figs. 7 and 8. (a) v_1^I, v_4^I, and v_6^I vs. v_2^I curves are identical to v_1^{II}, v_4^{II}, and v_6^{II} vs. v_2^{II} curves. (b) v_3^I and v_5^I vs. v_2^I curves differ from v_3^{II} and v_5^{II} vs. v_2^{II} curves.

$$R_1 = R_4 = 0, \quad R_2 = R_5, \quad R_3 = R_6.$$

The closure equations of this 6*R* linkage could be different from Eq. (17) after introducing non-zero offsets, which needs further study.

Because of the similarity between the non-symmetrical Bennett-joint 6*R* linkage and Case II linkage, the non-zero offsets for the former may be applicable to the latter, too, i.e.

$$R_1 = R_4 = 0, \quad R_2 = R_6, \quad R_3 = R_5.$$

Again the closure equations for non-zero offsets need to be derived.

Both of the newly found linkages have collinear configurations, making them ideal a building blocks for construction of large expandable structures. In particular, because of the nature that they are formed from

Bennett linkages, they can be seamlessly slotted into the assemblies of Bennett linkages that were reported in [16], enabling the creation of rapidly deployable arches and towers for emergency or military operations.

Acknowledgements

Y. Chen would like to thank the Nanyang Technological University, Singapore, for providing a research grant (RG21/05) and subsequent academic leave to undertake works related to this article. Z. You would like to express his gratitude to the Royal Academy of Engineering for giving him a Global Research Award, which enabled this work to be completed. He was also awarded a visiting scholarship by Dalian University of Technology when preparing the manuscript.

References

[1] G.T. Bennett, A new mechanism, Engineering 76 (1903) 777–778.
[2] F.E. Myard, Contribution à la géométrie des systèmes articulés, Societe Mathématiques de France 59 (1931) 183–210.
[3] M. Goldberg, New five-bar and six-bar linkages in three dimensions, Transactions of ASME 65 (1943) 649–663.
[4] C. Mavroidis, B. Roth, Analysis and synthesis of overconstrained mechanism, in: Proceedings of the 1994 ASME Design Technical Conference, Minneapolis, MI, September, 1994, pp. 115–133.
[5] P. Dietmaier, A new 6*R* space mechanism, in: Proceeding 9th World Congress IFToMM, Milano, vol. 1, 1995, pp. 52–56.
[6] K. Wohlhart, Merging two general Goldberg 5*R* linkages to obtain a new 6*R* space mechanism, Mechanism and Machine Theory 26 (2) (1991) 659–668.
[7] Y. Chen, Design of structural mechanism, Ph.D. thesis, University of Oxford, 2003.
[8] Y. Chen, J.E. Baker, On using a Bennett linkage as a connector between other Bennett loops, Proceeding of Institution of Mechanical Engineers, Journal of Multi-body Dynamics 219 (2) (2005) 177–185.
[9] J.E. Baker, On generating a class of foldable six-bar spatial linkages, Transactions of the ASME, Journal Of Mechanical Design 128 (2006) 374–383.
[10] K.J. Waldron, Hybrid overconstrained linkages, Journal of Mechanism 2 (1968) 73–78.
[11] J.E. Baker, The Bennett, Goldberg and Myard linkages – in perspective, Mechanism and Machine Theory 14 (1979) 239–253.
[12] C.R. Calladine, Buckminster Fuller's "tensegrity" structures and Clerk Maxwell's rules for the construction of stiff frames, International Journal of Solids and Structures 14 (1978) 161–172.
[13] C.R. Calladine, S. Pellegrino, First-order infinitesimal mechanisms, International Journal of Solids and Structures 27 (4) (1991) 505–515.
[14] Y. Chen, Z. You, T. Tarnai, Threefold-symmetric Bricard linkages for deployable structures, International Journal of Solids and Structures 42 (8) (2005) 2287–2301.
[15] J.E. Baker, An analysis of Bricard linkages, Mechanism and Machine Theory 15 (1980) 267–286.
[16] Y. Chen, Z. You, Mobile assemblies based on the Bennett linkage, in: Proceedings of the Royal Society A (Mathematical, Physical and Engineering Sciences), vol. 461, 2005, pp. 1229–1245.